Ultracold dipolar bosons trapped in quantum circuits

Author: Joan Pelegrí Andrés
Facultat de Física, Universitat de Barcelona, Diagonal 645, 08028 Barcelona, Spain.

Advisor: Muntsa Guilleumas

Abstract: We study a Bose-Hubbard trimer populated with an ultracold gas of dipolar bosons. By exact diagonalization of the many-body Hamiltonian, we analyze different cases, depending on the strength of the interactions that take place amongst the bosons and their polarization.

I. INTRODUCTION

Since 1995, when the first Bose-Einstein condensate was obtained [1], the experimental techniques in this field have developed enormously. Nowadays, a myriad of different systems can be built and tested, which has lead to a large expansion of the field [2].

In this work, we will simulate a particular system known as Bose-Hubbard (BH) trimer, which consists of three potential wells amongst which tunneling is allowed. We will consider it to be populated with an ultracold gas of dipolar bosons. In contrast to the isotropic short-range contact interaction usually present in ultracold gases, dipole-dipole interactions are anisotropic and long-range. This opens the possibility for new physics, which has been recently developed [3].

II. DESCRIPTION OF THE SYSTEM

In order to describe this system, we will follow a similar approach to that of Ref. [4]. We will consider that all the dipoles, each one corresponding to one boson, are oriented in the same direction. Each potential well (or site) will be identified by a number (1,2,3). We will focus on the case for which the tunneling rate between all pairs of sites is the same.

In addition to that, we will also take into account the interatomic interaction. This interaction has two components, an on-site one, which corresponds to the interaction between bosons that are in the same potential well, and an intersite one, which corresponds to the interaction amongst the bosons that are located in different potential wells. The on-site interaction is due to a combination of dipolar and s-wave contact interactions. As a first approach, we will consider this interaction to be pair-wise. The intersite one is due to the long range character of the dipolar interaction. We will consider that each group of bosons located in the same site create an effective dipole, which corresponds to the superposition of all of them. Then, the intersite interaction can be thought as the interaction amongst these effective dipoles.

For simplicity, we will work within the second quantization formalism. In our study, we will restrict to a subspace of the Fock space with the total number of particles, N, fixed.

Taking all these features in consideration together with the form of the dipolar interaction [4], the Hamiltonian of the system reads:

$$\hat{H} = -J(\hat{b}_1^\dagger \hat{b}_2 + \hat{b}_1^\dagger \hat{b}_3 + \hat{b}_2^\dagger \hat{b}_3 + h.c.) + \frac{U_{on}}{2} \sum_{i=1}^{3} \hat{n}_i(\hat{n}_i - 1) + U_{int} \sum_{i<j} (1 - 3\cos^2\theta_{ij}) \hat{n}_i \hat{n}_j \,, \quad (1)$$

Where $\hat{b}_i^\dagger$, $\hat{b}_i$ and $\hat{n}_i = \hat{b}_i^\dagger \hat{b}_i$ are the creation, annihilation and number bosonic operators of each site, respectively [5]. J, U_{on} and U_{int} are characteristic parameters of the system which control the tunneling rate, the on-site interaction and the intersite one, respectively. J an U_{int} are positive defined, whereas U_{on} can be either positive (repulsive interaction) or negative (attractive interaction). θ_{ij} is the angle between the direction that joins each pair of effective dipoles (each corresponding to one site) and the direction of polarization.

The general procedure that we will carry out in order to study this system is to build the matrix representation of the Hamiltonian (1) in the Fock basis of our subspace, i.e. $F_3 = \{|n_1, n_2, n_3\rangle \mid n_1 + n_2 + n_3 = N\}$, and then diagonalize it. From the diagonalization we can obtain the energy spectrum and the wave function of any state we might be interested in, which in general will be the ground state (GS). The diagonalization will be carried out numerically, using a function which relies upon the Implicitly Restarted Lanczos Method [6].

Once the wave function of the state that we want to analyze is obtained, we can characterize several relevant features of that state, such as expected values of different observables or entanglement properties. The latter will be obtained by means of a bipartite splitting, that is, by tracing the density matrix of the state that we are analyzing with respect the Fock basis corresponding to 2 sites, populated with at most N particles in total, i.e. $F_2 = \{|i, j\rangle \mid i + j \leq N\}$. This can lead up to three different reduced density matrices, one for each site. It can be proven that, for any state, in the Fock subspace in which we will be working, these reduced density matrices are always diagonal in the $F_1 = \{|0\rangle, ..., |N\rangle\}$ basis, see Ref. [7]. Therefore they will read:

$$\rho^{(i)} = \mathrm{Tr}_{\mathrm{j,k}}(\rho) = \sum_{l=0}^{N} \lambda_l^{(i)} |l\rangle \langle l| \,, \quad (2)$$

with $i, j, k = 1, 2, 3$.

The λ_l coefficients are known as the entanglement spectrum. As a general property, they fulfill $\sum_l \lambda_l = 1$. From them, the Schmidt gap ($\Delta\lambda$) and the von Neumann entropy (S), which are two figures of merit that characterize the entanglement of a particular state, can be computed.

The Schmidt gap is defined as the difference between the two largest λ_l coefficients. When $\Delta\lambda^{(i)} = 1$, it means that the state considered is a product state with respect to site i, i.e. $|\psi\rangle = |\psi\rangle_i \otimes |\psi\rangle_{j,k}$. The von Neumann entropy is defined as $S = -\sum_l \lambda_l \log \lambda_l$. A large von Neumann entropy corresponds to large entanglement, and vice versa. Its largest value is reached for $\lambda_l = 1/(N+1)\,,\ \forall l$ and its minimum when one of the coefficients equals one, i.e. $\Delta\lambda = 1$. In order to normalize it to 1, we will take the logarithms in base $N+1$.

III. RESULTS

In order to understand better all the results obtained, it might be helpful to first take a look at the intersite interaction term of the Hamiltonian. As it is seen in (1), concerning each pair of sites there is a coefficient multiplying it: $U_{int}(1 - 3\cos^2\theta_{ij})$. U_{int} is positive defined, so, for each pair of sites, the attractive or repulsive character of this interaction depends entirely on the value of θ_{ij}. If this angle is such that $1 - 3\cos^2\theta_{ij}$ is positive, the interaction will be repulsive, whereas if it is negative, it will be an attractive one. As limiting cases, we note that $\theta_{ij} = \pi/2$ is the most repulsive case and $\theta_{ij} = 0$ the most attractive one.

It is also interesting to note that, due to the tunneling term of the Hamiltonian, the matrix representation of $\hat{H}$ is never diagonal in the F_3 basis. This fact makes the generic ground state of the system to be $|\psi\rangle_{GS} = \sum_{n_1,n_2} C_{n_1,n_2} |n_1, n_2, N - (n_1 + n_2)\rangle$, which in general is not an eigenstate of the number operators, $\hat{n}_i$.

Keeping these features in mind, we will start by studying the ground state of some characteristic configurations, depicted in Fig. 1. In the α and β configurations, a clear symmetry and equivalence between sites 1 and 3 can be observed, whereas in the the γ configuration the symmetry is amongst all sites.

Fixing the total number of bosons $N = 48$, we solve the Hamiltonian (1) by exact diagonalization. We will first look at the different phases that appear depending on the values of the on-site and the intersite interaction coefficients, for each characteristic configuration.

A. α configuration

As seen in Fig. 1 (left panel), in the α configuration we have $\theta_{12} = \theta_{23} = \pi/6$ and $\theta_{13} = \pi/2$. Therefore, there is attraction between sites 1-2 and 2-3, but repulsion between 1-3. In Fig. 2, we show the average occupations

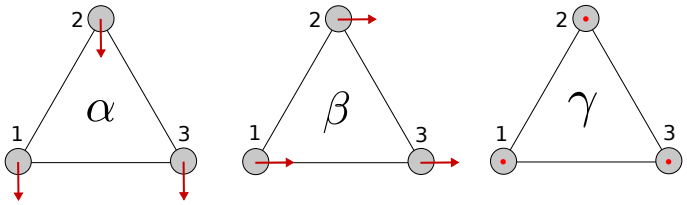

FIG. 1: Schematic representation of α, β and γ configurations. The vectors show the polarization of the effective dipoles for each configuration. However, its length is not related to their strength, as each site can be populated with a different number of bosons.

of site 1 and 2 for the ground state. We can clearly distinguish three phases:

Phase $\alpha.a$. The on-site attractive interaction, which in this region is stronger than the inter-site one, tends to group all the bosons in the same site. For the on-site interaction all the sites are equivalent, so it does not prioritize the occupation of any of them. However, as the occupation of only one site does not take place (due to the tunneling part of the hamiltonian), the intersite interaction plays a role, prioritizing the occupation of site 2 as it is more stable in the alpha configuration.

Phase $\alpha.b$. We see that in this region, the expected occupation of site 1 is granulated, but the occupation of site 2 is well defined. In general, granulated regions in expected occupation diagrams correspond to a degeneracy in the energy spectrum. Indeed, we have obtained that in this case the ground state of the system is two-fold degenerated. In order to understand this result, we note that the dominating interaction is the intersite one. Thinking about the properties of this configuration, we can see that the system tends to the following expected occupations in order to minimize its energy in the $J \to 0$ limit: $\langle\hat{n}_2\rangle$, $\langle\hat{n}_1\rangle \to N/2$ and $\langle\hat{n}_3\rangle \to 0$, or $\langle\hat{n}_2\rangle$, $\langle\hat{n}_3\rangle \to N/2$ and $\langle\hat{n}_1\rangle \to 0$. These two configurations are equivalent and degenerated. Therefore, by exact diagonalization, we can reach any superposition of them. As $\langle\hat{n}_2\rangle \to N/2$ is the same for both, it is well defined, but the expected occupations of

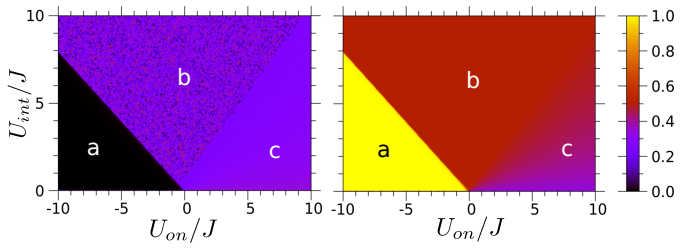

FIG. 2: Expected average occupations, $\langle\hat{n}_1\rangle/N$ (left) and $\langle\hat{n}_2\rangle/N$ (right) in the $(U_{int}/J,\ U_{on}/J)$ plane for the ground state of the system in the α configuration. These results have been obtained for $N = 48$.

sites 1 and 3 are not. For the latter ones, due to this superposition, we reach any random number (always respecting $\langle\hat{n}_1\rangle+\langle\hat{n}_2\rangle + \langle\hat{n}_3\rangle = N$).

Phase $\alpha.c$. In this case, the on-site repulsive interaction is stronger than the intersite one, thus it dominates. The on-site repulsive one, tends to distribute the particles uniformly in the three sites, as discussed in Ref. [7]. Therefore, we expect to have approximately the same particles in each potential well, but with a correction due to the intersite interaction. As the interaction between sites 1-3 is repulsive and attractive otherwise, we observe a depletion of sites 1 and 3, and an increase of the expected number of bosons in site 2. It can be seen that this depletion and increase is progressive, the more intense the intersite interaction, the more significant this phenomena becomes.

B. β configuration

In this configuration, the characteristic angles are $\theta_{12} = \theta_{23} = \pi/3$ and $\theta_{13} = 0$, as depicted in Fig. 1 (middle panel). Thus, there is attraction between sites 1-3 and repulsion otherwise. This case turns out to be the opposite of the α configuration. From the numerical results obtained, depicted in Fig. 3, we can again distinguish three phases:

Phase $\beta.a$. In this region there is a two-fold degeneracy in the ground state. Because of that, this phase appears granulated in the average expected occupation of site 1. Basically, this can be explained noticing that the on-site interaction dominates and it is attractive, meaning that it tends to gather all the bosons in one site. The intersite interaction acts as a correction to this distribution. Due to the features of the beta configuration and the tunneling part of the Hamiltonian, the less energetic configurations are either $\langle\hat{n}_2\rangle, \langle\hat{n}_1\rangle \to 0$ and $\langle\hat{n}_3\rangle \to N$, or $\langle\hat{n}_2\rangle, \langle\hat{n}_3\rangle \to 0$ and $\langle\hat{n}_1\rangle \to N$, as site 2 is the only one that feels intersite repulsion with all the others. These two degenerated limiting configurations explain the results obtained.

Phase $\beta.b$. In this region, the intersite interaction dominates. From the β configuration features, it follows that in this case, in order to minimize its energy, the system has to populate only sites 1 and 3. Looking at the Hamiltonian of the system (1), we see that the magnitude of the intersite interaction is proportional to the product $\hat{n}_i\hat{n}_j$, so the energy is minimized when the expected occupation of site 1 and 3 is the same. This matches with the results obtained: $\langle\hat{n}_1\rangle, \langle\hat{n}_3\rangle \to N/2$ and $\langle\hat{n}_2\rangle \to 0$.

Phase $\beta.c$. The on-site interaction dominates. In this case it is repulsive, which means that tends to distribute the bosons equally amongst the three sites. The intersite acts then as a correction to this distribution, slightly unbalancing the expected occupation in sites 1 and 3 with respect to 2, as there is attraction between site 1 and 3 and repulsion otherwise. As it can be seen, this unbalancing becomes more significant the more intense the intersite interaction is.

C. γ configuration

As commented before, in this configuration all sites are equivalent, so the same physics is observed for the three of them. This is due to the fact that $\theta_{12} = \theta_{13} = \theta_{23} = \pi/2$, as it can be seen in Fig. 1 (right panel). Moreover, this corresponds to the case of maximum repulsion between all pairs of sites. Looking at the results depicted in Fig. 4, we can distinguish two different phases:

Phase $\gamma.a$. This phase corresponds to the region where the on-site attractive interaction dominates, as well as to the region in which the intersite interaction does. In both cases, the interaction amongst bosons basically tends to group them in a single site, their effect is equivalent. Due to the total equivalence amongst the three sites, we obtain three-fold degeneracy in the ground state, and the granulated expected occupation associated to it.

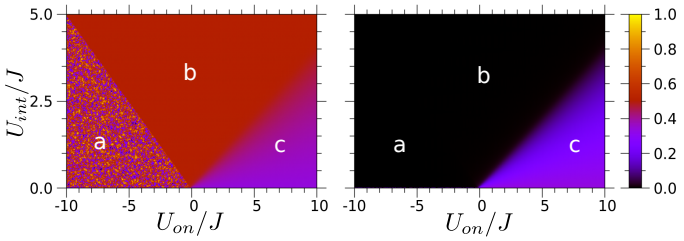

FIG. 3: Expected average occupations, $\langle\hat{n}_1\rangle/N$ (left) and $\langle\hat{n}_2\rangle/N$ (right) in the $(U_{int}/J, U_{on}/J)$ plane for the ground state of the system in the β configuration. These results have been obtained for $N = 48$.

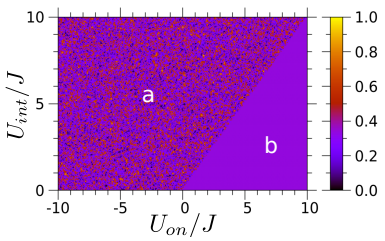

FIG. 4: Expected average occupation of site one, $\langle\hat{n}_1\rangle/N$, in the $(U_{int}/J, U_{on}/J)$ plane for the ground state of the system in the γ configuration. These results have been obtained for $N = 48$.

Phase $\gamma.b$. The on-site interaction dominates. In this case it is repulsive, which means that tends to distribute the bosons equally amongst the three sites. As in this case all the sites are equivalent, it does not unbalance the configuration, and the expected average occupation of each site in the ground state is the same for all of them: $\langle \hat{n}_1 \rangle$, $\langle \hat{n}_2 \rangle$, $\langle \hat{n}_3 \rangle \to N/3$.

D. General case

In the previous sections, we have obtained the same results as in Ref. [4]. Now we will consider a new scenario, in which all the possible orientations of the dipoles are permitted, fixing the interaction coefficiens.

We choose the y-axis to be in the direction that joins sites 1 and 3. We represent the direction of the dipoles with a generic unit vector expressed in spherical coordinates. Computing the corresponding scalar products, we can reach the following expressions for the cosines squared that are involved in the dipolar interaction:

$$\begin{aligned}
\cos^2\theta_{13} &= (\sin\theta\sin\phi)^2 \\
\cos^2\theta_{12} &= (\sin\theta\sin\phi)^2\left[\sin\left(\frac{\pi}{3}\right)\mathrm{cotg}\,\phi - \cos\left(\frac{\pi}{3}\right)\right]^2 \\
\cos^2\theta_{23} &= (\sin\theta\sin\phi)^2\left[\sin\left(\frac{\pi}{3}\right)\mathrm{cotg}\,\phi + \cos\left(\frac{\pi}{3}\right)\right]^2 .
\end{aligned}$$

From these expressions, we can see that this interaction is symmetric with respect to $\theta = \pi/2$, and invariant under π-shifts of ϕ. Thus, studying the system in the $\theta - \phi$ plane with θ only ranging from 0 to $\pi/2$ and ϕ from 0 to π, we can already observe all the phenomenology of this general case.

A useful way of exploring this new situation is to decompose the dipolar vectors in two components; their projection to the plane of the trimer and the one perpendicular to it. The former will vary its orientation only with respect to ϕ, passing through different characterisitic configurations which we can identify with the α and β ones, as it is schematically shown in Fig. 5. On the other hand, the latter components will always have the same orientation, which corresponds to a γ configuration. Varying θ, we can control the magnitude of each contribution. We can range from the case of having the dipolar vectors in the plane of the trimer ($\theta = \pi/2$) to the one in which they are perpendicular to it ($\theta = 0$).

Having a closer look at Fig. 5, we can also notice that the phenomenology observed in each site has to be the same as that of the other sites within $\pi/3$ shifts of ϕ (forwards or backwards), since our choice of axis has been totally arbitrary. We could have associated $\phi = 0$ to a α_3 or a α_1 configuration instead of a α_2, and yet the system would be the same. It is because of this equivalence that we shall only focus on the phenomena observed in one site.

As an illustrative case, we will consider a strong intersite interaction, without on-site one. In particular, we will consider $U_{on} = 0$ and $U_{int}/J = 5$. The results obtained are depicted in Fig. 6, from which we can distinguish different phases:

Phases A_i. This phases appear for low values of θ, where the γ-like components of the dipoles dominate. As there is no on-site interaction, they tend to gather the bosons in one site. In fact, the effect of this components alone has been already characterized in $\gamma.a$ phase. Now, however, for most of the ϕ values, the dipolar components parallel to the plane of the trimer break completely the three-fold degeneracy observed in the $\gamma.a$ phase, promoting the occupation of site i with respect to the others. This is due to the fact that these components make one site more stable, except when the β_{i-j} configurations in the plane of the trimer are reached. These configurations make two sites equally stable, and therefore a two-fold degeneracy in the energy spectrum is found. These par-

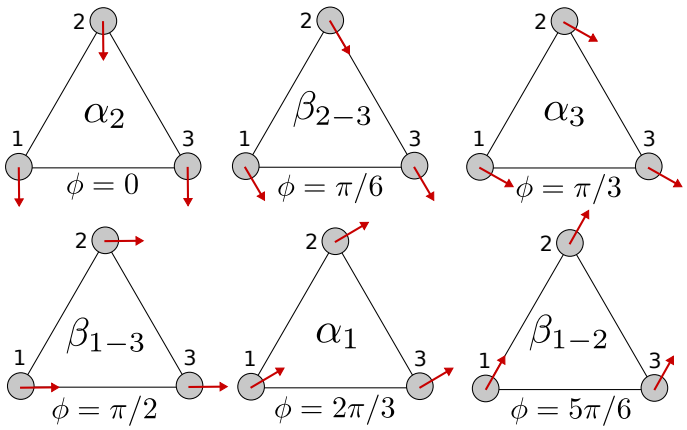

FIG. 5: Schematic representation of the characteristic configurations reached by the components of the dipolar vectors parallel to the plane of the trimer as a function of ϕ. The subscripts indicate the sites which each configuration tends to populate with more bosons, analogously as in the previous sections.

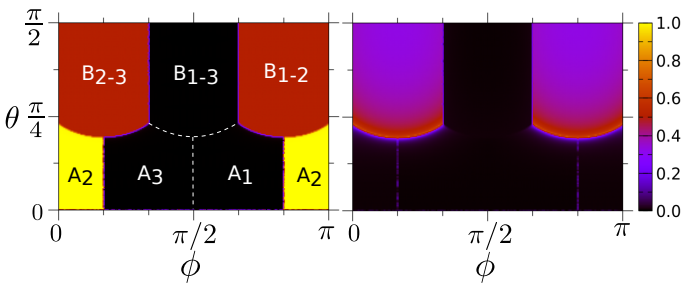

FIG. 6: Expected average occupation of site 2, $\langle \hat{n}_2 \rangle / N$, (left) and von Neumann entropy measured in site 2, $S^{(2)}$, (tracing with respect to sites 1 and 3) (right) for the ground state of the system. Although they are different magnitudes, they share the same scale. The results are shown in the (θ, ϕ) plane, and have been obtained for $U_{on} = 0$, $U_{int}/J = 5$ and $N = 48$.

ticular cases serve as the boundaries of the A_i phases.

Recalling the equivalence between a dominating γ-like intersite interaction and a on-site attractive one observed in phase $\gamma.a$, it is easy to see the analogy between phases A_i and the $\alpha.a$ phase. This analogy is also valid between the boundaries (β_{i-j} configurations in the plane of the trimer) and the $\beta.a$ phase.

Phases B_{i-j}. Now the components of the dipolar vectors parallel to the plane of the trimer dominate. In these phases there is equal expected occupation of only two sites. The particular cases for which α_i configurations in the plane of the trimer are reached define the boundaries between them.

These results can be understood thinking that, except for the α_i configurations, there is always a pair of sites for which the attraction is larger than the others. This situation is similar to that of $\beta.b$ phase. For the same reason, equal expected occupation of two stites and almost null occupation of the third is obtained. Therefore, we can establish again an analogy between phases B_{i-j} and $\beta.b$ phase. As for the boundaries (when α_i configurations in the plane of the trimer are reached), we can identify them with $\alpha.b$ phase.

The effect of varying θ in B_{i-j} phases can be appreciated in the von Neumann entropy, although it is not seen in the expected occupation of the sites, which remains constant. We see that the more intense the components perpendicular to the plane of the trimer are, the larger the entropy becomes.

In Fig. 7 different cuts of the entanglement spectrum are shown. In the left panel we have fixed $\theta = \pi/4$. In this cut, we can see that the Schmidt gaps tend to $\Delta\lambda^{(i)} \to 1$ in the B_{j-k} phase, but they are clearly different from 1 in the B_{i-k} and B_{i-j} phases. Therefore, B_{j-k} phases tend to a product state between site i and the other two, which remain entangled, as it was expected.

In the right panel, with $\phi = \pi/12$ fixed, we can also see the tendency $\Delta\lambda^{(i)} \to 1$ for the A_i phase. Noticing that total expected occupation of one site and null occupation of the others can only be reached with one of the Fock states: $|N,0,0\rangle, |0,N,0\rangle$, or $|0,0,N\rangle$, we can infer that the Schmidt gaps measured in the other sites tend to one as well. Therefore, A_i phases tend to a product state between the three sites.

Moreover, we see that the entanglement spectrum collapses in the phase transitions. This phenomena has also been found in Refs. [4] and [7], and it serves as a way of identifying those transitions.

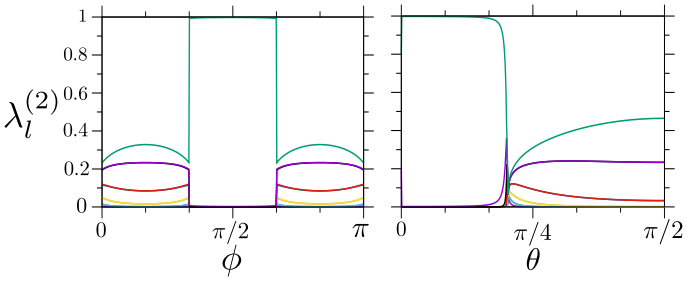

FIG. 7: Entanglement spectrum of the ground state of the system measured in site 2 as a function of ϕ, for $\theta = \pi/4$ fixed (left), and as a function of θ, for $\phi = \pi/12$ fixed (right). Both spectra have been obtained for $U_{on} = 0$, $U_{int}/J = 5$ and $N = 48$.

IV. CONCLUSIONS

We have studied the anisotropic effects of the dipolar interaction in the ground state of a BH trimer populated with dipolar bosons, obtained by exact diagonalization of the many-body Hamiltonian. First, by considering three characteristic configurations, we have seen how the competition between the on-site interaction and the intersite one leads to different phases. After that, we have considered a different scenario, in which all the orientation of the dipoles are permitted, but the strength of the interactions is fixed. In all the cases, we have seen how the orientation of the dipoles plays a crucial role, due to the anisotropy of the dipolar interaction.

We have shown that the different phases numerically obtained can be characterized by means of expected average occupations and energy degeneracy. In the general case, we have also seen that the entanglement properties of the system can be very helpful in these characterizations.

Acknowledgments

I would like to thank Muntsa Guilleumas and Bruno Juliá for their orientation and discussions about the subject, which have made all this project possible.

[1] Eric A. Cornell, Carl E. Wieman *The Bose-Einstein condensate*, Scientific American (1998).
[2] I. Bloch, J. Dalibard, and W. Zwerger, Rev. Mod. Phys. 80, 885 (2008).
[3] T. Lahaye, C. Menotti, L. Santos, M. Lewenstein, T. Pfau, Rep. Prog. Phys. 72, 126401 (2009).
[4] A. Gallemí, M. Guilleumas, R. Mayol and A. Sanpera, New J. Phys. A 88, 063645 (2013).
[5] W. H. Dickhoff, D. Van Neck *The many-body theory exposed!*, World Scientific Publishing Co. Pte. Ltd. (2005)
[6] https://docs.scipy.org/doc/scipy-0.14.0/reference/generated/scipy.sparse.linalg.eigsh.html
[7] A. Gallemí, M. Guilleumas, J. Martorell, R. Mayol, A. Polls and B. Juliá-Díaz, New J. Phys. 17 073014 (2015).